ISSN 1063-7826, Semiconductors, 2008, Vol. 42, No. 5, pp. 531–539. © Pleiades Publishing, Ltd., 2008.
Original Russian Text © V.G. Bozhkov, N.A. Torkhov, I.V. Ivonin, V.A. Novikov, 2008, published in Fizika i Tekhnika Poluprovodnikov, 2008, Vol. 42, No. 5, pp. 546–554.

## SEMICONDUCTOR STRUCTURES, INTERFACES, AND SURFACES

# Study of the Properties of the Surface of Gallium Arsenide by Scanning Atomic Force Microscopy

**V. G. Bozhkov[a], N. A. Torkhov[a]^, I. V. Ivonin[b], and V. A. Novikov[b]**

[a]*OAO Research Institute of Semiconductor Devices, ul. Krasnoarmeiskaya 99-a, Tomsk, 634050 Russia*

*^e-mail: trkf@mail.ru*

[b]*Tomsk State University, pr. Lenina 36, Tomsk, 634050 Russia*

Submitted September 11, 2007; accepted for publication September 24, 2007

**Abstract**—Using the method of atomic force microscopy, complex studies of the profile, potential distribution $\varphi(x, y)$, and distributions of the phase contrast of the surface of *n*-GaAs subjected to various types of chemical treatment are carried out. The distribution of the potential and phase contrast at a microlevel, in general, correlates with the profile character. The surface treated in the solution $H_2SO_4 : H_2O = 1 : 10$ is characterized by a high degree of nonuniformity with an average roughness of the main profile $\Delta h \approx 10$ nm. A considerable part of the surface is covered by hills 20–60 nm in height and 100–500 nm in diameter forming a specific substructure, which correspond to potential jumps as large as 50–60 mV against a general background of 0.77–0.80 V. At a nanolevel, correlation between the profile and phase contrast is clearly pronounced, but no correlation is found between the profile and potential distribution. Treatment of the surface of *n*-GaAs in a concentrated aqueous $NH_4OH$ solution leads to a decrease in the value of $\varphi(x, y)$ by ~0.2 V, and in its roughness by more than an order of magnitude (~0.75 nm). The distribution of the profile and phase contrast over the surface is close to the ideal Gaussian distribution for relatively small areas of the surface ($200 \times 200$ nm$^2$). As the area increases, deviation from the Gaussian distribution becomes substantial because of smooth variation in the potential over the contact area. Conservation of the Gaussian character of the surface profile and a simultaneous rise in the average level of the roughness with an increase in the analyzed area indicates the fractal mechanism of formation of the surface profile.

PACS numbers: 68.47.Fg, 68.37.Ps, 73.61.Ey, 68.35.Ct, 61.43.Hv, 68.55.-a

**DOI:** 10.1134/S1063782608050084

## 1. INTRODUCTION

Many problems of microelectronics, and especially nanoelectronics, are directly related to the formation of semiconductor structures with a clean and uniform surface of a sufficiently large area. This applies to GaAs. In the ideal, we keep in mind the fabrication of an atomically clean and atomically smooth surface. However, the actual attainment of this purpose in laboratory and especially production conditions meet a number of difficulties. They are associated with the development of both the methods of treatment and cleaning of the semiconductor surface and the methods of sufficiently simple and effective control of the state of the surface, namely, the structure, composition, profile, and potential. In the last two decades, considerable achievements have been made in both directions. Particularly, the methods of scanning atomic force microscopy not only provide important information on the properties of the surface at the nanolevel, but also become more available in practical development.

In some studies (see, for example, [1]), it has been shown that the use of concentrated hydrochloric acid in solutions of ethanol and isopropanol with $pH < -1$ leads to the formation of amorphous arsenic on the GaAs surface, from fractions of a monolayer to one to three monolayers thick, depending on the preliminary state. This layer can be rather simply removed by heating in ultrahigh vacuum at $T \leq 400$°C in order to obtain virtually atomically clean surface. However, in production practice, treatments that are more accessible are used [2]; such treatments give quite satisfactory results, for example, for the fabrication of the micrometer-size Schottky-barrier contacts. This is indicated by the rather high quality of their current–voltage (*I–V*) and other characteristics [3]. However, the problem of improvement of characteristics of the Schottky-barrier contacts (in very different applications) and increasing their sensitivity and stability is rather urgent, especially when going to the region of submicrometer sizes, and is largely limited by the quality of preparation of the surface and its control in the process of device fabrication.

In connection with the aforesaid, the purpose of this study was to use scanning atomic force microscopy (AFM) to gain insight into the state of the surface (profile, phase contrast, and potential) of epitaxial GaAs subjected to various treatments used in practice for fabrication of Schottky-barrier metal–semiconductor contacts.

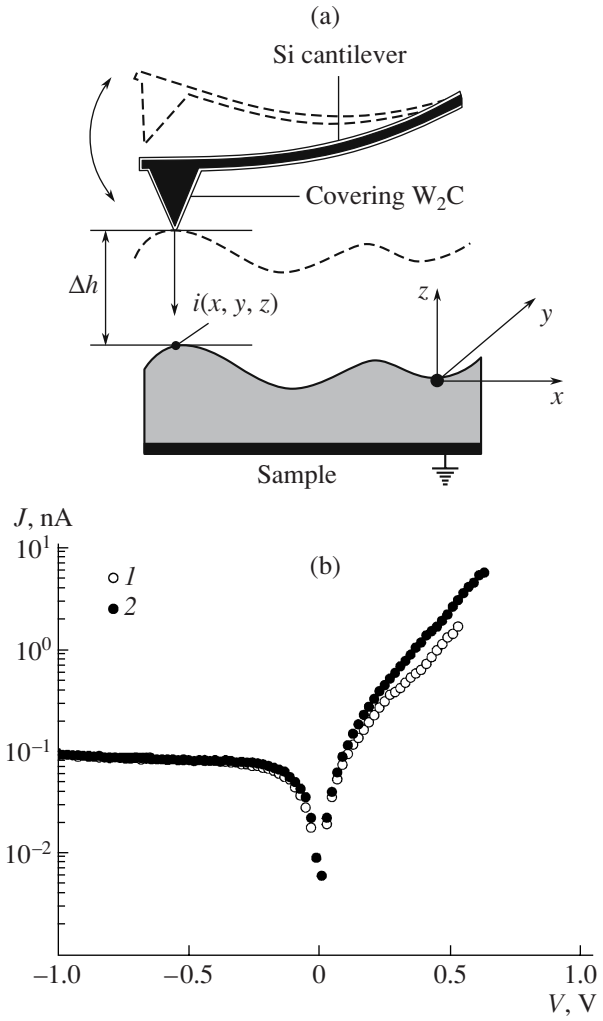


**Fig. 1.** (a) Schematic representation of the operation of the atomic force microscope in the two-passage mode and (b) current–voltage characteristics recorded using a scanning probe (tip of the cantilever needle) by a contact method in two various points of the surface marked by symbols *1* and *2*.

## 2. EXPERIMENTAL

We studied the structures $n$–$n^+$-GaAs:Sn (100) obtained by MOC-hydride epitaxy with an epitaxial layer 0.3 μm thick and a concentration of dopant in the $n$-layer of $6 \times 10^{16}$ cm$^{-3}$. The structures passed a standard processing itinerary (itinerary 1). This involved the preliminary chemical cleaning (mainly for degreasing) via sequential treatments in monoethanolamine ($C_2H_7ON$), dimethylformamide ($C_3H_7ON$), and isopropanol ($C_3H_7OH$). To remove native oxides, we used treatment in the solution $H_2SO_4 : H_2O = 1 : 10$ (pH = –0.5) for 10 s (counteretch). Then, prior to fabrication of the ohmic contact to the substrate, the epitaxial layer was protected by a silicon oxide ($SiO_2$) layer 100 nm thick, which was deposited plasmochemically (by decomposition of monosilane) at $T = 280$°C. The ohmic contact, which is necessary for performance of precision AFM studies, was fabricated after removal of the traces of deposition of $SiO_2$ in a 5% HF solution and 30 μm of the substrate in the etchant $H_2SO_4 : H_2O_2 : H_2O = 3 : 1 : 1$. Fabrication of the ohmic contact involved the electrochemical deposition of the AuGe alloy (0.2 μm), its firing in the hydrogen atmosphere for 5 min at 450°C, and subsequent deposition of a gold layer 0.2 μm thick. Then insulator was removed from the front surface in a buffer etchant (HF : $NH_4F$ (40%) : $H_2O$ = 15 : 115 : 31 volume fractions) with subsequent rinsing in deionized water for 2 min. As the finish treatment, which is usually used immediately prior to deposition of barrier contacts, we used counteretch of the surface (see above) and washed in isopropanol.

Itinerary 2 differed from itinerary 1 only in the finishing treatment of the surface, where ammonia treatment was used instead of counteretch. The former involved treatment in a concentrated (25%) aqueous solution of $NH_4OH$ (pH = 12) and washing in isopropanol.

Studies of the surface were carried out using a Solver-NDT commercial atomic force microscope (AFM), which provided the measurement of the surface profile, potential distribution over the surface, and its phase contrast [4–6]. The scanning step was determined by the selection of linear sizes of the scanned region and by the used number of steps ($256 \times 256$).

Measurements were carried out in air under standard conditions in a semicontact operation mode with the use of a two-passage procedure. For operation in the semicontact mode, we used Si cantilevers of the NSG10/$W_2C$ type, which comprised a micromechanical facility consisting of a beam 35 μm in width, 60 μm in length, and 2 μm in thickness mounted on a support (Fig. 1a). At the free end of the beam, on its lower surface, a tip with radius $r = 35$ nm covered with a solid current-carrying $W_2C$ coating 30 nm thick was formed. Operation in the semicontact mode implies oscillation of the cantilever tip at a resonance frequency of the beam $\omega_z$. The two-passage procedure implies twice-repeated passage (scanning) of the same scan line by the tip.

During the first passage, mechanical oscillations of the beam at the resonance frequency $\omega_z$ are excited by piezoelectric elements. The measurement of the surface profile (coordinate of the $i$th point of the surface $i(x, y, z)$) of the sample is performed by the feedback signal, which is determined by the travel of the beam tip in the $(xy)$ plane and by the variation in the amplitude of its vibrations $A_{iz}(\omega_z)$ along the $z$ axis in the instant of touching the surface with the tip.

Simultaneously with plotting the image of the spatial surface profile during the first passage, the image of its phase contrast is plotted. During scanning of the surface in the semicontact mode, a periodic variation in the oscillation phase θ at each impingement of the tip of the cantilever needle with the surface caused by the interaction of the needle with the surface substance takes

place. The image of the surface of the phase contrast comprises the distribution of the phase variation $\Delta\theta$ in the $(x, y)$ plane. The variation in $\Delta\theta$ is caused by different properties of segments of the surface, with which the needle interacts (microhardness, viscosity, plasticity, etc.), which in practice reflects the variation in the phase composition of the surface. In a two-dimensional image of the phase contrast, the same variation in $\theta$ (homogeneity of the phase composition) is characterized by one shade of gray. Therefore, the distribution of the shade of gray in the $(x, y)$ plane will give a qualitative pattern of spatial distribution of the physical properties of the surface.

During the repeated passage of the cantilever, after the measurement of the surface profile and phase contrast, the potential profile of the surface is measured. For this purpose, the cantilever tip is lifted over the surface for a distance $\Delta z$. To excite the oscillations of the tip, the ac voltage (signal) is applied directly to the probe–sample system in this case. The frequency of the ac voltage (signal) is selected equal to the resonance frequency $\omega_z$, which provides isolation and measurement of only the electric component of the force $F_z$ acting between the sample and cantilever.

The force of electrical interaction $F_{iz}$ between the $i$th point of the sample surface and the tip of the cantilever needle is determined by the gradient of energy $E$ accumulated by the capacitance of this system $C_i$ ($E = C_i U_i^2/2$):

$$F_{zi} = -\frac{\partial E}{\partial z} = -\frac{1}{2}U_i^2\frac{\partial C}{\partial z}. \quad (1)$$

Here, $U_i(z)$ is the potential difference between the $i$th point of the surface and the cantilever, which involves the surface potential with respect to the grounded contact $\varphi_i(x, y)$, an external weak ac signal with amplitude $U_1$ and frequency $\omega_z$, and the constant (compensating) voltage $U_0$:

$$U = U_0 - \varphi_i(x, y) + U_1\sin(\omega_z t). \quad (2)$$

Substituting (2) into (1), we can easily isolate the measured harmonic component of the interaction force:

$$F_{zi}(\omega_z) = -\frac{1}{2}\{[U_0 - \varphi_i(x, y)]U_1\sin(\omega_z t)\}\frac{\partial C}{\partial z}. \quad (3)$$

From the balance condition $F_{zi}(\omega_z) = 0$, we determine the potential $\varphi_i(x, y)$ equal to the external compensating voltage $U_0$.

Since $\partial C/\partial z$ considerably increases as the distance decreases, the optimal condition for carrying out the measurements is the condition $\Delta z < r$.

Figure 1b shows the $I$–$V$ characteristics of the probe–sample ($W_2C$–$n$-GaAs) system for the point touching of the surface by the needle tip for two different points. Despite the fact that the radius of such contact is small and comparable with the radius of the tip of the cantilever needle equal to 35 nm, the shape of represented $I$–$V$ characteristics corresponds to the type of the diode $I$–$V$ characteristic of the Schottky-barrier metal–semiconductor contact. This circumstance directly indicates that there exists a potential barrier in the probe–sample system, a part of which, in a general case, is the contact potential difference or the surface potential $\varphi_i(x, y)$ [7].

Notice that the surface was scanned with a fixed number of steps (points, pixels) $N = 256 \times 256$ irrespective of the scanned area.

## 3. RESULTS AND DISCUSSION

Although the preliminary history of formation of the surface is undoubtedly important, it is evident that the finishing processes exert the most profound effect on its state. In our case, this is removal of silicon oxide in a buffer etchant, treatment in the aqueous solution of sulfuric acid, and short-term rinsing in deionized water (itinerary 1). It is known (see, e.g., [8]) that acidic solutions (pH < –0.3) dissolve oxides of GaAs. For this purpose, solutions not only of sulfuric acid but also of hydrochloric acid ($HCl : H_2O = 1 : 1$, pH = –0.7) are used [9–11]. Subsequent rinsing in deionized water removes the products of dissolution and traces of the solution itself, but also stimulates oxidation of the surface [8]. For this reason, short-term rinsing is used. As a result, the surface is formed, on which the presence of oxides of gallium and arsenic is not just possible [8] but is really observed (see, e.g., [12]).

Figure 2 shows the images obtained using AFM measurements of (a) the surface profile, (b) surface potential, and (c) phase contrast of epitaxial $n$-GaAs layer passed the standard chemical treatment (route 1). The bottom part of each of the images represents the relief profiles of these images corresponding to the sections marked by dashed lines. Let us at once notice the well-pronounced correlation between all three characteristics of the surface as concerns the characteristic hills (islands) 20–60 nm in height and 100–500 nm diameter on a relatively smooth surface of $n$-GaAs (Fig. 2a). These hills correspond to potential jumps of 20–40 mV against the background of its relatively smooth variation (Fig. 2b) and clearly pronounced variations in the phase composition (Fig. 2c). The correlation between the phase contrast and surface profile is also confirmed by the comparison of their profiles (see dashed line in Fig. 2c): the profile peaks correspond to valleys in the phase contrast, although the pattern of the phase contrast looks like more complex. We can state that the described hills (islands), in general, differ by the phase composition and form a specific substructure, which uniformly covers the entire surface of the epitaxial $n$-GaAs layer. There are strong grounds to associate the presence of the surface roughness (and other features of the profile) with the treatment's character. For example, this is indicated by comparison with the similar results of the study of the GaAs surface after

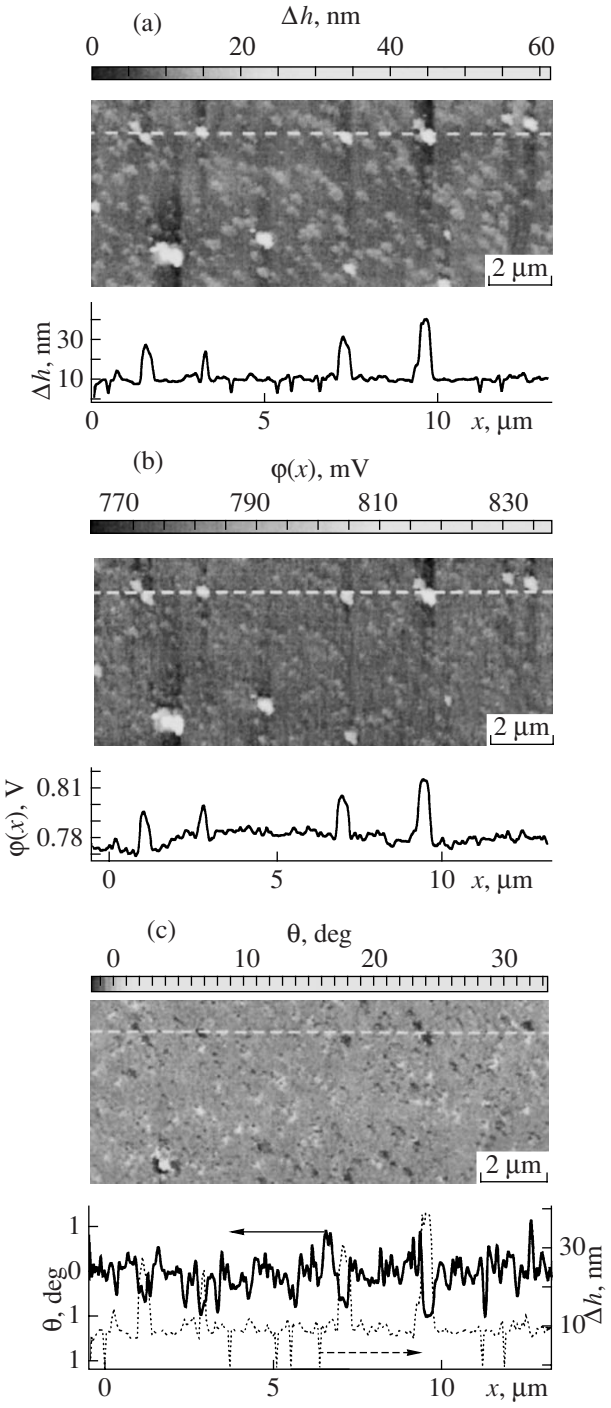


**Fig. 2.** AFM images of the segment ($13.3 \times 13.3\ \mu m^2$) of the surface of the epitaxial *n*-GaAs layer treated by route 1. (a) Spatial profile and its transverse section, (b) potential profile of the surface and its transverse section, and (c) phase contrast of the surface profile and its transverse section. The dashed line in Fig. 2c reproduces the profile $\Delta h(x)$ in Fig. 2a.

removal of silicon oxide by etching in a buffer etchant. It turned out that in the last case, the profile does not contain a considerable amount of hills (which unambiguously associates their emergence with counteretch), and the level of the surface roughness (see below) is substantially lower than after counteretch.

The main smoother surface profile (between the hills) corresponds to the roughness $\Delta h \approx 10$–15 nm. Separate pits as deep as 10 nm and with the transverse section as large as 100 nm are clearly pronounced (Fig. 2a). The surface potential in this region varies rather smoothly (Fig. 2b). Oscillations amount to 10–20 mV over areas of hundreds of square micrometers, and potential fluctuations at the nanolevel are even lower. It is difficult to discuss the correlation between the profiles of potential, roughness, and phase contrast at the nanolevel. We can only notice that the pits (or pores) found at the spatial profile do not noticeably manifest themselves in the potential profile.

At a high resolution (Figs. 3a, 3b), it is evident that the surface profile of *n*-GaAs and the phase contrast are formed by the layer of rather uniform grains adjacent to one another. These grains (especially in the image of the phase contrast) have clearly pronounced boundaries and relatively small oscillations in size (50–100 nm in diameter, 10–15 nm over the height). It is interesting that the prominent islands of the profile in Fig. 3a, similarly to the regions outside of them, also have a grain structure with the difference that their grains are accumulated into three-dimensional clusters (aggregates), which distinguish them against the background of the main profile. In Fig. 3b, the image of the phase contrast in the region of islands and outside of them differs rather weakly. However, the qualitative correlation between the profile and the phase contrast is clear: it is evident that the profile peaks in Fig. 3a correspond to rather clearly outlined regions of the phase contrast.

In the bottom part of Figs. 3a and 3b, the profiles of roughness and phase contrast corresponding to the mentioned sections (*1*) and (*2*) are represented. The sections are selected so that one of them passes through the prominent island (*2*), and the other one passes through the region of the main smooth surface profile (*1*). The surface profiles look smoother, excluding certain abrupt valleys apparently caused by pores, which reflects the oval form of the grains. In the profiles of the phase contrast, a relatively flat part corresponds to the regions of grains, which reflects the homogeneity of the phase, and the valleys correspond to their boundaries. The deepest valleys also possibly correspond to the pores. Under close examination, it is easy to verify the correlation of both profiles for section (*1*) (Fig. 3a): grain boundaries correspond to jumps of the phase contrast. With respect to section (*2*), it is more difficult to make such a conclusion, since the profile is substantially roughened because of the presence of a rather high hill. In general, we can state that although interpretation of the phase contrast has a qualitative character, it gives important additional information with respect to not only the phase composition but also the geometric structure of surface features.

It is noteworthy that the AFM method is rather widely used for the study of the surface profile of semiconductors. However, the data on studies of the phase contrast and potential distribution over the surface are rather limited. Results of the study of the GaAs surface qualitatively similar to Figs. 2a and 3a were reported in [12], although due to different histories of the surface, the quantitative parameters of the profile substantially differ. Based on the results of [12] and others [2, 8, 13], we can state that the surface profile of GaAs is formed preferentially by oxides of gallium and arsenic. Based on the represented results, we can assume that the presence of hills, by virtue of correlation of their location with the distribution of the surface potential, is associated with the presence of active segments on the surface (where the negative charge is localized), which promote acceleration of oxide growth.

A general notion of the complexity of the profile, surface potential, and phase contrast of the surface is given by corresponding bar graphs presented in Fig. 4. The main part of the images are approximated by three bar graphs, which can be conventionally prescribed to three main phase-structural features on the surface. According to what is expected from the analysis of the equilibrium state of the system in contact with acidic solutions and water [8], these can be oxides of arsenic and gallium and elemental arsenic, although more complex formations are not excluded. We can notice the presence of rather pronounced distribution tails. A large part of them corresponds to relatively large-sized features (hills with $\Delta h > 20$ nm) with an increased potential and phase contrast. The additional complexity of interpretation of the potential bar graphs is the fact that smooth variation in the potential on the surface, probably associated with the nonuniformity of bulk properties, is superposed on a general pattern. As for the bar graph of the phase contrast, it is given mainly for completeness of the pattern, since its immediate physical interpretation is still difficult.

Let us add to the aforesaid that the left-hand part of the distribution is probably affected by dark strips near the structural hills (Fig. 2a), which are associated with methodical features of the image formation near abrupt hills and pores.

A drastic variation in the state (primarily, composition) of the GaAs surface can be attained by treatment in clearly pronounced alkaline (pH ≥ 13) and acidic (pH < –1) media, in which not only dissolution of native oxides but also their effective removal from the surface are possible. In this case, only elemental arsenic can be present in the equilibrium on the GaAs surface [8]. Such an abrupt variation in the surface state should lead to an identically abrupt variation in its characteristics. In this study, for this purpose, we used the finishing treatment of the surface in a concentrated $NH_4OH$ aqueous solution (ammonia treatment), after which the sample was placed into isopropanol, heated until boiled, and dried in its vapors for 5 min (see route 2). In such a medium, the earlier present native oxides are effectively dissolved and removed from the surface [8].

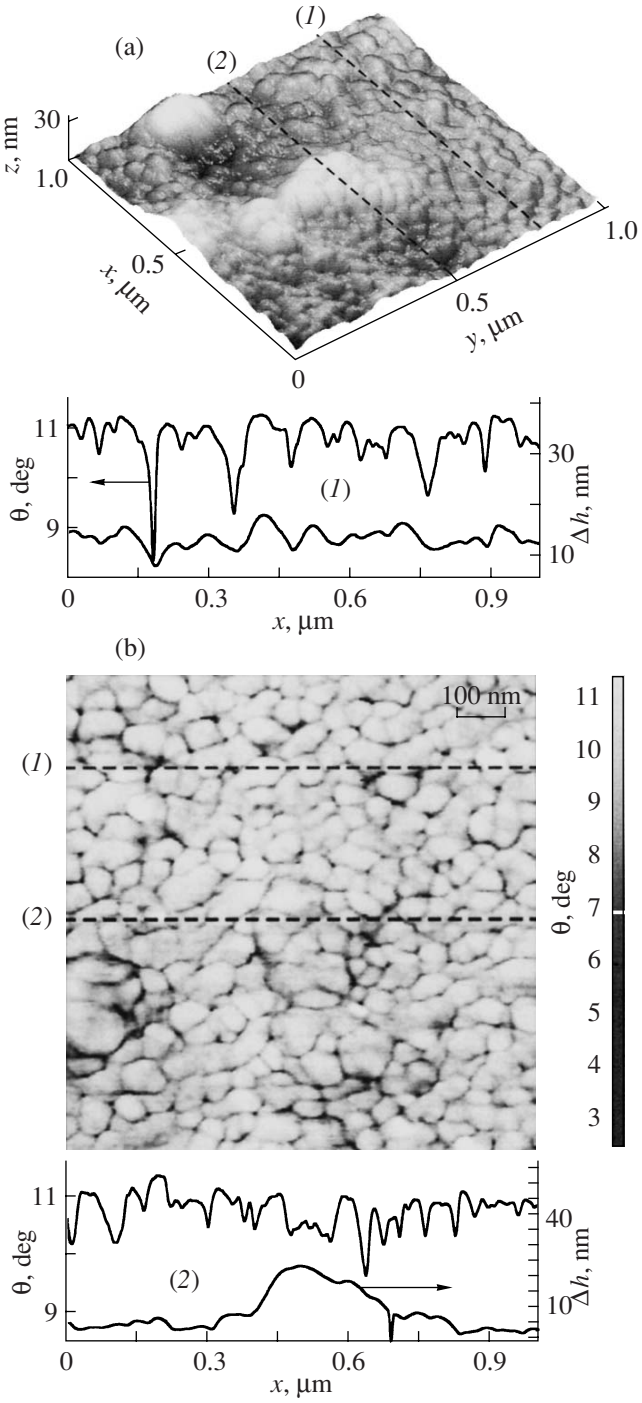


**Fig. 3.** AFM images of the segment ($1 \times 1$ μm$^2$) of the surface of the epitaxial *n*-GaAs layer treated according to route 1. (a) Three-dimensional spatial profile and its transverse section and (b) phase contrast of the surface profile and its transverse section.

It follows indeed from Figs. 5 and 6 that the state of the GaAs surface changes drastically. First of all, hills

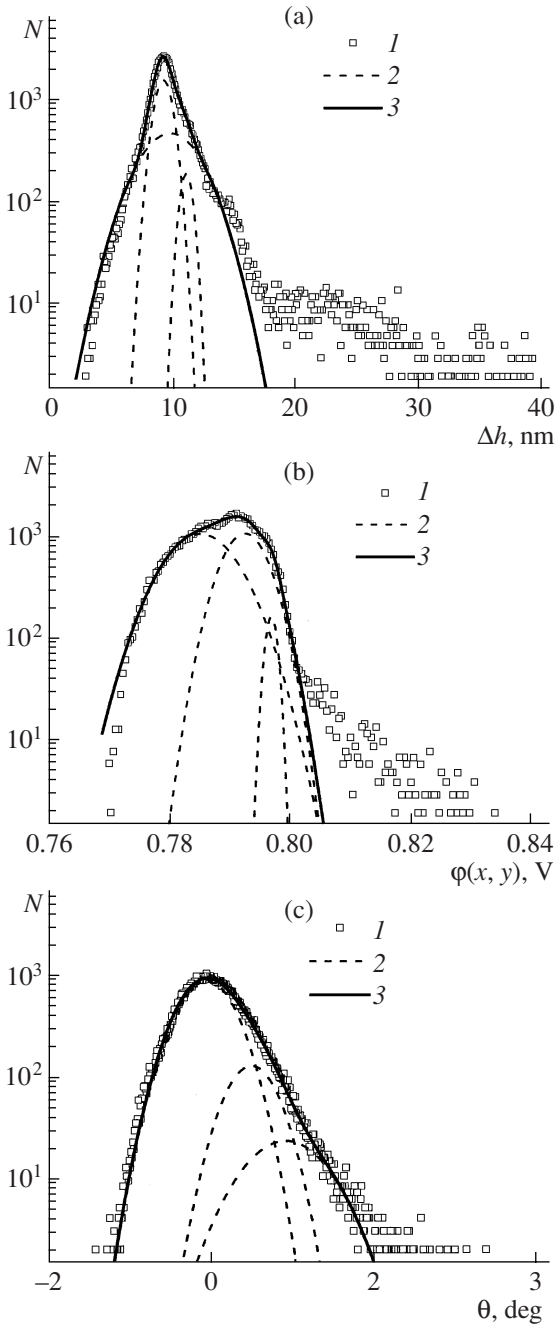


**Fig. 4.** (a) Bar graphs of the distribution of the roughness $\Delta h$ of the spatial surface profile represented in Fig. 2a (route 1), (b) bar graph of the distribution of the potential of this surface $\varphi(x, y)$, and (c) bar graph of the phase contrast. Points correspond to experimental values (*1*), dashed lines correspond to approximation by the Gaussian functions (*2*), and solid lines correspond to the sum of the Gaussian functions (*3*).

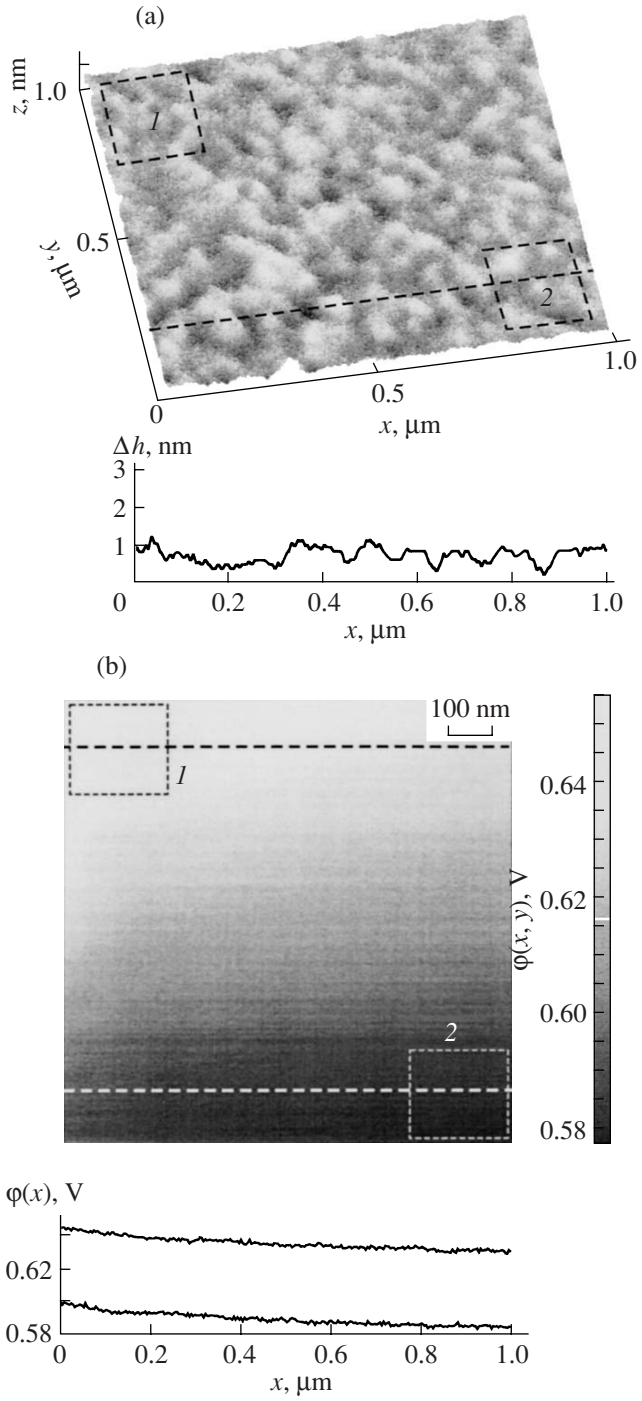


**Fig. 5.** AFM images of the segment ($1 \times 1$ μm$^2$) of the surface of the epitaxial *n*-GaAs layer treated by route 2. (a) Three-dimensional spatial profile and its transverse section and (b) potential profile of the surface and its transverse section.

of the microprofile (island formations) and the corresponding potential peaks disappear. The surface roughness decreases virtually by an order of magnitude (Fig. 5a). Similarly, fluctuations of the potential (Fig. 5b) and phase contrast (Fig. 6a) decrease (profiles of images presented in their bottom part correspond to sections marked by dashed lines). An additional substantial variation is a decrease in the surface potential by approximately 0.2 V. A smooth variation in the potential is noticeable (Fig. 5b). Its causes are apparently associated with the effect of bulk forces for the samples selected for the study.

One interesting circumstance should be noted. The variation in the surface potential due to the treatment, which initiates the emergence of elemental arsenic on the surface, is consistent with interpretation of the variation in the barrier height in the model of Spicer et al. [14–16]. According to the conclusions of these authors, an increase in the As content in the near-surface region and, consequently, an increase in the concentration of $As_{Ga}$ centers as compared to $Ga_{As}$ centers should shift the Fermi level to a level 0.75 eV, one of two donor levels emerging on the surface during deposition of metal. The barrier height in the M–*n*-GaAs contact (M is metal) should decrease in this case. In contrast, a decrease in the concentration of $As_{Ga}$ centers should shift the Fermi level to a level 0.5 eV, i.e., to increase the barrier height in the contact. It is evident that in our case, a decrease in the surface potential completely corresponds to a decrease in the effect of As in the M–*n*-GaAs contact.

It follows from Figs. 5a and 5b (and especially from comparison of the roughness and potential profiles) that correlation between the surface profile and potential distribution is absent. However, in this case, we can also discuss the correlation of the roughness and phase contrast of the surface, as it follows from comparison of their profiles in Fig. 6. Its presence once more confirms the natural relation between the profile of the surface and its phase contrast, which we mentioned when analyzing Fig. 3.

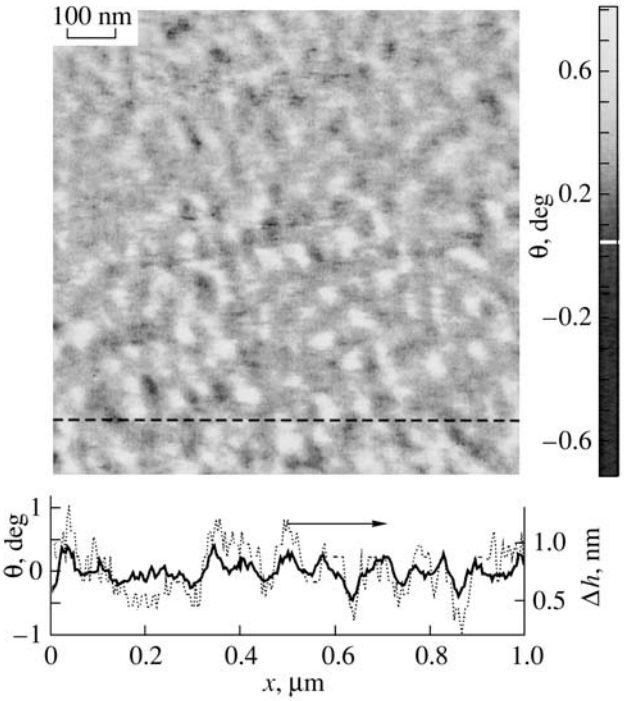


**Fig. 6.** Image of the phase contrast of the surface profile of the segment $1 \times 1$ μm$^2$ of the epitaxial *n*-GaAs layer treated by route 2 and its transverse section.

Statistical processing of the data of the profile (Fig. 7a) shows that the last one is ideally described by a Gaussian distribution peaked at $\Delta h \approx 0.76$ nm. Practically the same can be applied to the distribution of the phase contrast (Fig. 7c), which once more indicates their connection. The potential distribution is considerably more complex (Fig. 7b), but the cause for this is evident: the rather strong and smooth variation in the potential mentioned above (Fig. 6b). For segments *1* and *2* with approximately uniform shade of the image selected in Fig. 6b, potential distributions are close to the Gaussian one (Fig. 8).

Let us note another interesting result. The Gaussian distribution for the surface profile is retained virtually in the same form as in Fig. 7a, and for separately taken surface segments *1* and *2* in Fig. 8. This fact possibly indicates that the characteristic size ~0.76 nm is the minimal size for this profile. The point is that, as the analyzed area increases, the Gaussian distribution is still in effect, but the characteristic size that corresponds to the distribution peak rises. For the area $10 \times 10$ μm$^2$ it amounts to 2.51 nm, while for the area $99 \times 99$ μm$^2$ it is 7.52 nm. This circumstance allows us to conclude that the profile character corresponds to a fractal mechanism of its formation, which is widely used for the description of the profile of metallic and other surfaces [13, 17].

In the general case, the surface is considered to be fractal if it consists of parts which are similar to the whole in a certain sense [18]. The main characteristic of fractal surfaces is the value of their fractal dimensionality $2 < D_f < 3$, which exceeds the value of topological dimensionality of the surface under study ($D_t = 2$) by definition and therefore is a fractional quantity. No true fractal surfaces exist in nature. Actual surfaces can be only self-affined, i.e., can possess the property of similarity in a rather narrow range of measuring scales δ. According to performed estimates [13], for the epitaxial *n*-GaAs layer, the value of δ can vary in the limits from hundredth fractions to tens of nanometers.

In this study, in order to determine $D_f$ of the surface of the epitaxial *n*-GaAs layer, we used the triangulation method [18]. Calculation of the value of $D_f$ by the triangulation method consists of the sequential approximation of the surface by the set of pyramids and measurement of the area of their lateral surfaces. In this case, the accuracy of the measurement of the surface area *S* depends on the number of such pyramids (number of divisions), which is determined by the magnitude of the measuring scale δ. As for the fractal (self-affined) surface, the quantities *S* and δ are related by the expression [18]

$$S = S_0 \delta^{2 - D_f}, \tag{4}$$

where $S_0$ is the area of the projection of the lateral surface on the $(x, y)$ plane. Therefore, by the slope of the linear portion of the dependence $\ln S = f(\ln \delta)$, it is easy to determine the value of $D_f$. Estimation of the value of fractal dimensionality of the surface performed by the

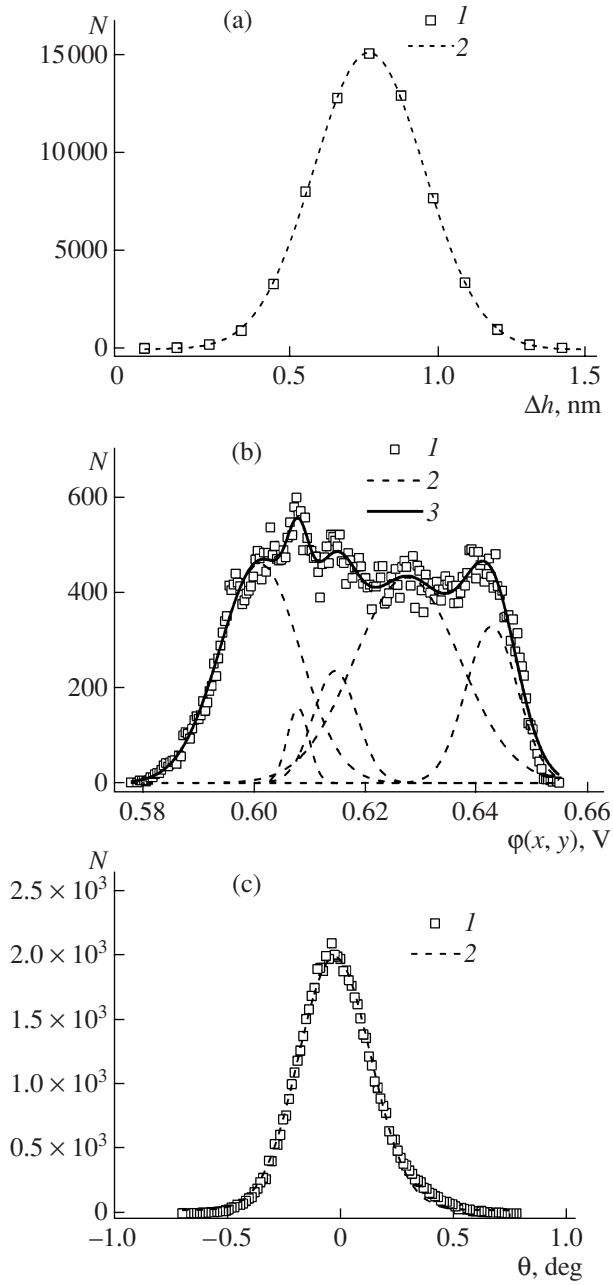


**Fig. 7.** Bar graphs of the distribution of the values of quantities: (a) roughness $\Delta h$ of the spatial surface profile represented in Fig. 5a (route 2), (b) potential of this surface $\varphi(x, y)$, and (c) phase contrast. (*1*) Experimental values, (*2*) approximation by the Gaussian functions, and (*3*) sum of the Gaussian functions.

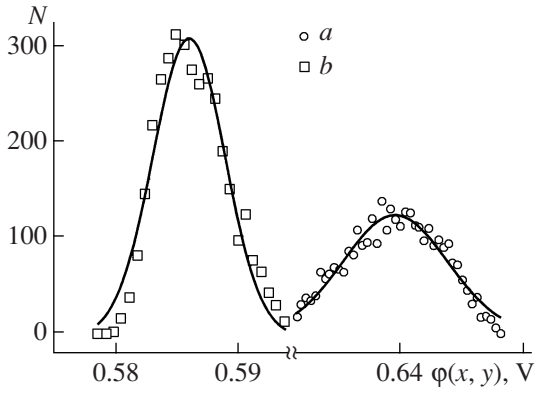


**Fig. 8.** Bar graphs of the distribution of the potential $\varphi(x, y)$ of isolated segments *1* and *2* of the surfaces of the potential profile (route 2) represented in Fig. 5b. Symbols *a* and *b* correspond to the experiment, and solid lines represent the approximation by the Gaussian functions. Symbols *a* show the data for segment *2* in Fig. 5 and symbols *b* show the data for segment *1* in Fig. 5.

triangulation method gave the value $D_f = 2.42 \pm 0.01$, which means a rather developed, specifically with a pronounced roughness, surface of the *n*-GaAs layer. A pronounced surface roughness of the epitaxial *n*-GaAs layer leads to a substantial increase in its surface area. For example, estimates of the actual surface area represented in Fig. 5a and based on expression (4) gave the value 10.27 μm$^2$, which is larger by an order of magnitude than the area of the scanned window (scan), equal to a mere 1 μm$^2$.

It is interesting that for the surface treated by route 1, the dependence of the average roughness on the size of the area under study is also observed. As a result, it is established that counteretch of the surface of the epitaxial *n*-GaAs layer leads to a lower value of $D_f = 2.19 \pm 0.01$. The lower value of the quantity $D_f$ indicates that, despite a large average surface roughness $\Delta h$ (roughness size), its actual area exceeds the scan area 1 μm$^2$ by a factor of only 2.87. Therefore, we can see that the value of fractal dimensionality of the semiconductor surface reflects not only the value of the average roughness but also the degree of roughness (the character of the roughness distribution over the surface).

## 4. CONCLUSIONS

For the first time, we used the AFM method to study in detail the profile, potential distribution, and distribution of the phase contrast of the *n*-GaAs surface subjected to various chemical treatments. The surface treated in an aqueous solution of sulfuric acid ($H_2SO_4$ : $H_2O$ = 1 : 10) for 10 s (counteretch) is characterized by a high degree of nonuniformity: the average roughness of the main profile amounts to $\Delta h \approx 10$ nm. In this case, a considerable part of the surface is covered by hills (islands) 20–60 nm in height and 100–500 nm in diameter, which form a specific substructure that uniformly covers the whole surface of the epitaxial *n*-GaAs layer. The relation of the profile with the character of the treatment is indicated by the fact that removal of silicon dioxide in a buffer etchant (prior to counteretch) is characterized by a surface roughness of GaAs lower by a factor of approximately 5 and by the absence of noticeable hills. The distribution of the potential and phase contrast in general correlates with the profile

character. Specifically, the profile peaks correspond to potential jumps (spikes) as large as 50–60 mV against a general background of 0.77–0.80 V. However, at the nanolevel, i.e., for the study of the segments with the sizes $1 \times 1$ μm$^2$, no noticeable correlation between the profile and potential distribution is found. Correlation of the profile and phase contrast is more pronounced. The latter, as is known, provides a clearer image of the profile.

The finishing treatment of *n*-GaAs surface in a concentrated aqueous $NH_4OH$ solution with pH = 12 (ammonia treatment) with subsequent rinsing in isopropanol, during which the native oxides are removed from the surface and the main product of interaction is elemental arsenic [8], gives a substantially different pattern of the profile, potential, and phase contrast. The absolute value of the surface potential decreases by ~0.2 V, and its roughness decreases by more than an order of magnitude. The same is related to the level of potential fluctuations. The distribution of the profile and phase contrast over the area is close to the ideal Gaussian distribution. The potential distribution corresponds to the Gaussian curve for relatively small segments of the surface ($200 \times 200$ nm$^2$). As the area increases, deviation from the Gaussian distribution becomes very substantial because of a gradual variation in the potential over the contact area.

The observed conservation of the Gaussian character of the surface profile with a simultaneous increase in the average roughness as the analyzed area increases is a reflection of the fractal mechanism of the formation of the surface profile.

## REFERENCES

1. V. L. Alperovich, O. E. Tereshchenko, N. S. Rudaya, et al., Appl. Surf. Sci. **235**, 249 (2004).
2. T. P. Bekezina and G. M. Mokrousov, Neorg. Mater. **36**, 1029 (2000) [Inorg. Mater. **36**, 867 (2000)].
3. V. G. Bozhkov, V. V. ViliSova, K. I. Kurkan, et al., Elektron. Promyshlennost' **9**, 82 (1993).
4. www.ntmdt-tips.com.
5. V. L. Mironov, *Fundamentals of Scanning Probe Microscopy* (Inst. Fiz. Mikrostruktur, Nizhni Novgorod, 2004) [in Russian].
6. A. D. Zimon, *Adhesion of Liquid and Wetting* (Khimiya, Moscow, 1974) [in Russian].
7. E. H. Rhoderick and R. H. Williams, *Metal–Semiconductor Contacts*, 2nd ed. (Clarendon, Oxford, 1988).
8. G. M. Mokrousov, *Transformation of Solids at Boundary of Solid Phases* (Tomsk. Gos. Univ., Tomsk, 1990) [in Russian].
9. H. Palm, M. Arbes, and M. Schulz, Phys. Rev. Lett. **71**, 2224 (1993).
10. G. M. Vanalme, L. Goubert, R. L. Van Meirhaeghe, et al., Semicond. Sci. Technol. **14**, 871 (1999).
11. S. Forment, R. L. Van Meirhaeghe, A. De Vrieze, et al., Semicond. Sci. Technol. **16**, 975 (2001).
12. D. Sadowska, A. Gładki, K. Mazur, and E. Talik, Vacuum **72**, 217 (2004).
13. N. A. Torkhov, Fiz. Tekh. Poluprovodn. **37**, 1205 (2003) [Semiconductors **37**, 1177 (2003)].
14. W. E. Spicer, T. Kendelewicz, N. Newman, et al., Appl. Surf. Sci. **33**, 1009 (1988).
15. W. E. Spicer, Z. Liliental-Weber, E. Weber, et al., Vac. Sci. Technol. B **6**, 1245 (1988).
16. W. E. Spicer, R. Cao, K. Miyano, et al., Appl. Surf. Sci. **41** (42), 1 (1989).
17. A. V. Panin and A. R. Shugurov, Poverkhnost' **6**, 64 (2003).
18. J. Feder, *Fractals* (Plenum, New York, 1988; Mir, Moscow, 1994).

*Translated by N. Korovin*